ELSEVIER

Journal of Power Sources 78 (1999) 54–64

JOURNAL OF POWER SOURCES

How compressible is recombinant battery separator mat?

Clive Pendry

Hollingsworth and Vose, Postlip Mills Winchcombe, GL54 5BB, England, UK

Abstract

In the past few years, the recombinant battery separator mat (RBSM) for valve-regulated lead/acid (VRLA) batteries has become the focus of much attention. Compression, and the ability of microglass separators to maintain a level of 'springiness' have helped reduce premature capacity loss. As higher compressions are reached, we need to determine what, if any, damage can be caused during the assembly process. This paper reviews the findings when RBSM materials, with different surface areas, are compressed under forces up to 500 kPa in the dry state.

Keywords: RBSM; VRLA; PCL; Compression; Separator

1. Introduction

In recent years, the battery industry has been actively attacking the problems of premature capacity loss (PCL) which has been defined as:

> the random failure of a positive plate by which the plate cannot return to or maintain its initial rated discharge capacity under cycling conditions.

PCL has been split into two areas:

– PCL1 due to a build up of a barrier layer around the grid/corrosion layer interface which has now been suppressed through the use of different grid alloys; and
– PCL2 due to the degradation of the bulk porous material [1–11] [12–20] [21–30] [31–39] [40–49] [50–58] [59–67] [68–70].

PCL 2 is of interest here, as compression and constraint of the porous material can be used to control the material expansion, maintaining the apparent density in the regions close to the grid, and, thereby preventing capacity loss, even under severe charge/discharge conditions.

Questions have been asked with respect to the ability of recombinant battery separator mat (RBSM) to withstand higher compressions whilst maintaining its compression resilience. It is well known that RBSM separators, when compressed, act like springs and oppose any further compression in the direction of the applied force. When the force is removed, the RBSM separator will recover to a point close to the starting point, making its action more like a viscoelastic material. A viscoelastic material deforms under stress over a period of time, showing a creep effect and can relax under a constant strain. One of many models for this type of action is the Maxwell–Kelvin model (Diagram 1—Maxwell–Kelvin model) [71]. This model uses Hookean spring to represent ideal elastic behaviour and Newtonian dashpots to represent viscose behaviour under the applied strain.

With this in mind, this study looks at a variety of different RBSM and modified RBSM separators to determine what effect the increased compressive forces have on the physical properties of tensile, elongation and compression recovery. Scanning electron microscope (SEM) work enables the inner structure of the separator materials to be examined for deviations from the normal.

Currently, this work has been conducted on separators in the dry state.

2. Experimental

A compression fixture designed and built by Hollingsworth and Vose (HV) [72] to work with the Instron tensile tester was used to compress a selection of different separators.

The effect of the forces was then determined by measuring the tensile strength and elongation of the uncompressed and compressed separators, along with viewing samples for structural changes using an SEM.

0378-7753/99/$ - see front matter
PII: S0378-7753(99)00011-7

Three Standard Hovosorb® RBSM separators with different surface areas (1.1 m^2/g, 1.25 m^2/g and 1.8 m^2/g) and four prototype organically modified separators, were cut into 100 mm × 100 mm squares for test under the pressure foot of the compression fixture.

The separator squares were loaded into the test fixture as shown. (Diagram 2—HV compression fixture). In total, five separator squares were tested during each test—two cut and tested in the machine direction (MD), two cut and tested in the cross-direction (CD) and one spared for SEM work. The spacers used between each separator square were of 100 mm × 100 mm × 8 mm stainless steel, thus preventing flexing during loading.

Three levels of compression were selected: 100, 250 and 500 kPa; this builds on previous work conducted at HV in the range of 2–146 kPa, using the BCI foot pattern of 29 mm diameter [73] in the dry and wet state. The results of this study have been shared with members of the EALABC and others on request. It demonstrates that at the two ends of the surface area spectrum, in the dry and wet state, standard RBSM materials still maintain a significant percentage of their compression and recovery character up to the 146 kPa maximum.

This report follows the JIS foot pattern being 100 × 100 mm [74] and covers a wider variety of separators. Initially, this study has been conducted in the dry state and all results are dry-state results. A follow-up study will show the wet state.

Three different rates of descent were tried—2 mm/min, 5 mm/min and 10 mm/min—to determine the effect of speed of compression.

The test duration was set at a maximum of 30 min. As the design matrix showed that a minimum of 34 sets of results were to be taken, this was seen to be the most manageable timeframe and close to the minimum time seen between assembly and filling.

On completion of the test, the stack was broken down.

The MD/CD tensile strength and elongation separator samples squares were cut into half before being tested on the Instron tensile tester. This operation was to ensure that the sample fitted the paper test jaws of the Instron, which have a grip of 50 mm.

The SEM sample was sent for coating and visual analysis under a selection of different magnifications from 250 to 2000 times.

3. Results

3.1. Physical Tests

The physical tests are split into three sections:
–tensile strength and elongation;

Table 1
Tensile strength/elongation

ESA/Grmg	Average tensile strength in stack machine direction—MD (kN/m)				Average tensile strength in stack cross direction—CD (kN/m)			
	Uncompressed	100 kPa	250 kPa	500 kPa	Uncompressed	100 kPa	250 kPa	500 kPa
1.1–188 g/m^2	0.44	0.43	0.35	0.42	0.31	0.30	0.28	0.26
1.1–366 g/m^2	0.59	0.50	0.31/0.56	0.16/0.41	0.47	0.41	0.28/0.44	0.12
1.1–400 g/m^2	0.64	0.61	0.56	0.45	0.47	0.47	0.44	0.40
1.25–183 g/m^2	0.43	0.46	0.49	0.40	0.31	0.30	0.33	0.27
1.25–201 g/m^2	0.58	0.45	0.28/0.55	0.17/0.38	0.40	0.31	0.21/0.42	0.11
1.25–351 g/m^2	0.91	0.89	0.85	0.83	0.62	0.65	0.69	0.64
1.8–233 g/m^2	0.87	0.77	0.58	0.25/0.76	0.66	0.62	0.41	0.20/0.64
Hovosorb-II-P-15: 278 g/m^2	1.69	1.52	1.68	1.61	1.03	1.06	0.83	1.04
H RDA 146 g/m^2	0.50	0.40	0.17	0.08	0.34	0.30	0.13	0.06
H RDB 217 g/m^2	1.14	0.98	0.90	0.71	0.99	0.84	0.72	0.64
H RDC 191 g/m^2	1.29	1.33	1.41	1.69	1.03	0.95	1.05	1.19
	Average elongation in stack machine direction—MD (%)				Average elongation in stack cross direction—CD (%)			
	Uncompressed	100 kPa	250 kPa	500 kPa	Uncompressed	100 kPa	250 kPa	500 kPa
1.1–188 g/m^2	3.05	2.84	2.28	3.31	6.68	5.87	5.97	6.07
1.1–366 g/m^2	2.48	2.83	3.00/2.21	2.35	4.61	4.42	5.37/4.43	3.06
1.1–400 g/m^2	2.24	2.77	2.57	2.28	3.36	3.67	4.00	4.72
1.25–183 g/m^2	2.15	2.33	2.51	2.18	4.28	4.34	4.97	3.89
1.25–201 g/m^2	3.45	3.46	3.47/3.24	2.63	7.20	6.49	6.4/5.16	3.95
1.25–351 g/m^2	2.81	2.62	2.85	2.80	3.32	3.74	4.83	4.54
1.8–233 g/m^2	2.16	2.45	2.73	1.69/1.73	4.65	4.91	4.27	3.18/4.53
Hovosorb-II-P-15: 278 g/m^2	4.21	5.49	3.82	3.09	4.21	5.63	3.68	3.77
H RDA 146 g/m^2	0.47	0.62	0.57	0.45	1.62	1.64	1.06	0.74
H RDB 217 g/m^2	2.00	1.81	2.94	5.43	3.38	3.36	4.19	8.56
H RDC 191 g/m^2	1.25	1.58	1.41	1.41	1.63	1.87	1.05	1.80

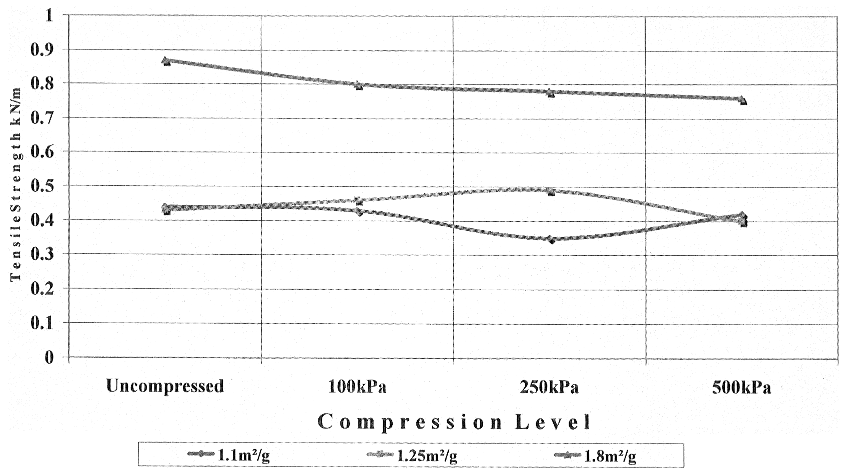

Fig. 1. Dry compressed tensile MD.

–compression characteristics; and

–SEM analysis.

Note: after the first three tests were conducted, the speed of compression was altered from 10 mm/min to 2 mm/min due to significant reductions in observed tensile strength at 250 and 500 kPa. This is highlighted in the results table where two results are shown in a cell. The first result is the original 10 mm/min test, the second, the 2 mm/min retest (Table 1).

Entrapped air movement through the separator voids has disrupted the structure.

3.1.1. Tensile strength—typical trends—Standard Hovosorb® RBSM

Irrespective of the surface area and grammage, the Standard Hovosorb® RBSM separators show a slight reduction in tensile strength as the force applied increases (Fig. 1).

If the recorded tensile strength values are compared against a typical paper manufacturing minimum of 0.19 kN/m for MD tensile strength, all but a couple of results are below this theoretical minimum at the 500 kPa level when the test speed was set to 10 mm/min. At the 10 mm/min rate, the samples drop to 28% of the initial tensile value, irrespective of surface area.

With the 2 mm/min test speed, the observed tensile strengths are more than acceptable, maintaining approximately 90% of the original tensile strength at 500 kPa.

3.1.2. Tensile strength—typical trends—Modified Hovosorb® separators

The H RDA sample was worse than a standard glass in all respects, which is a good example of how modification does not always improve the base material. In this case, the structural resilience has been totally disrupted (Fig. 2).

The H RDB sample has a tensile strength significantly better than the Standard Hovosorb® RBSM. Whilst the

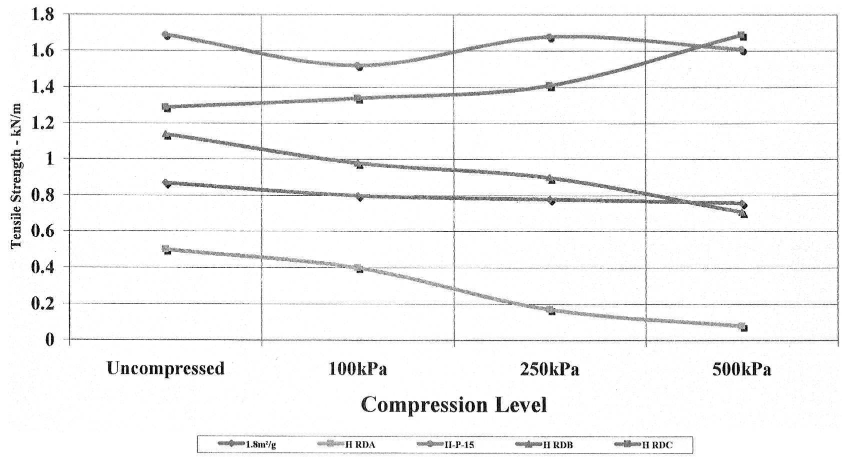

Fig. 2. Dry compressed tensile MD.

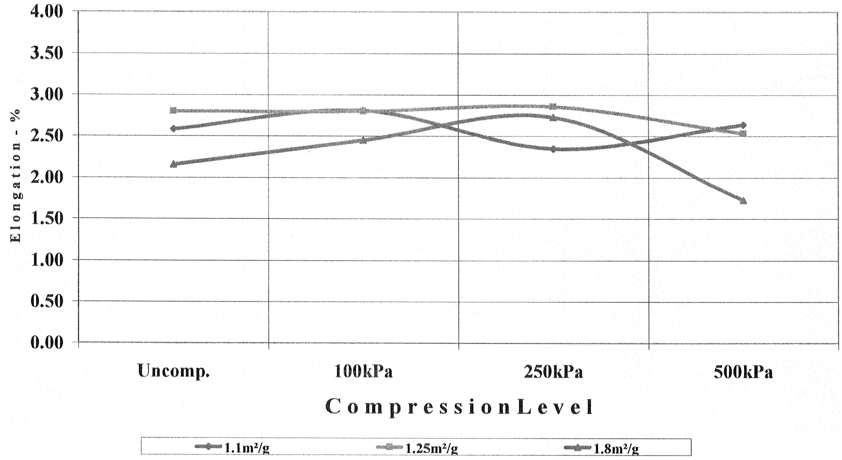

Fig. 3. Dry compressed elongation MD.

standard media show only a slight reduction in tensile strength, this modified separator has a definite downward trend on increased loading. Putting this into context, the 500 kPa result is similar to that observed for an uncompressed standard RBSM.

The H RDC sample improved in tensile strength as the force applied increased, which is a significant improvement over the standard material. This material is acting more like a perfect spring rather than a viscoelastic material. The tensile strengths observed at the start and end of the test are way above a standard RBSM material.

The Hovosorb®-II-P-15 maintained a constant tensile strength around the 1.6 kN/m region, irrespective of the force applied. This is significantly better than a pure RBSM.

3.1.3. Elongation—typical trends—Standard Hovosorb® RBSM

No pattern is apparent when looking at the elongation. Some samples increase in elongation and some samples decrease in elongation. Once again, these trends are independent of grammage and surface area in all cases. The 1.8 m^2/g sample has the lowest elongation of all the standard RBSM materials at the 500 kPa loading (Fig. 3).

3.1.4. Elongation—typical trends—Modified Hovosorb® separators

The H RDA reduces in elongation as the loading increases. The values are lower than any of the standard or Modified Hovosorb® separators. The standard glass matrix has been destabilised by the modifier, leading to reduced performance at the higher loading (Fig. 4).

The H RDB elongation increases significantly as the loading increases. This modified separator is becoming more elastic as the applied force increases.

The H RDC elongation values increase slightly over the uncompressed sample, but remain fairly constant, irrespective of loading.

The Hovosorb® II-P-15 has an elongation comparable to the standard RBSM material and is only beaten by the H RDB sample at 500 kPa.

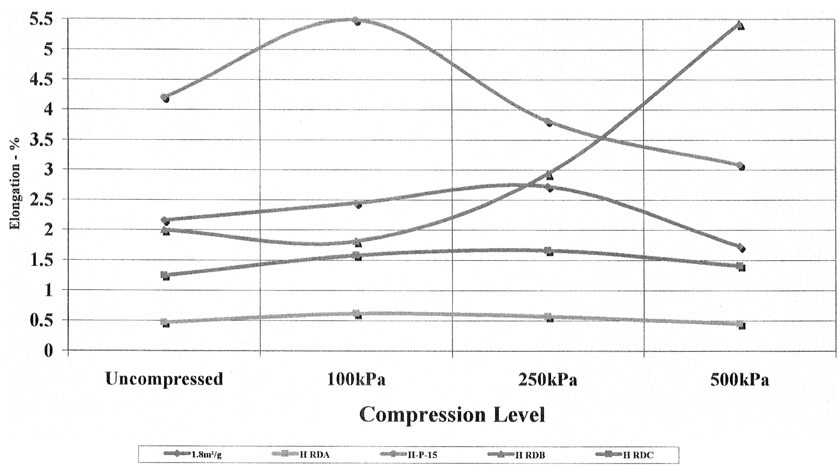

Fig. 4. Dry compressed elongation MD.

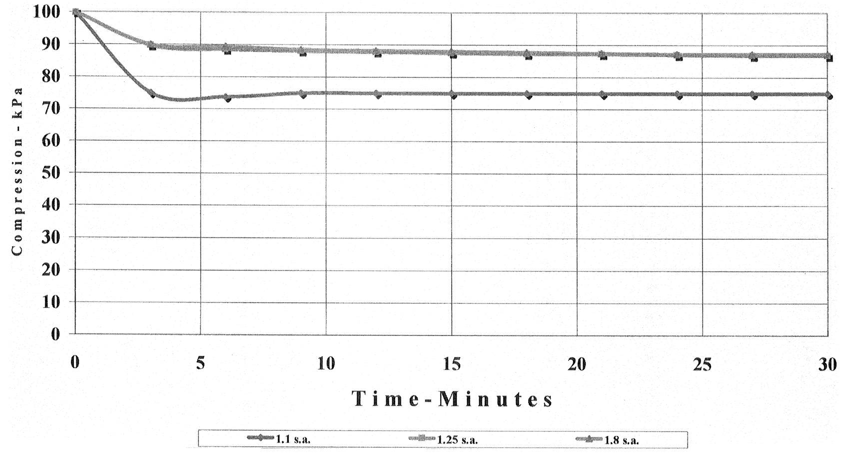

Fig. 5. Dry compression at 100 kPa.

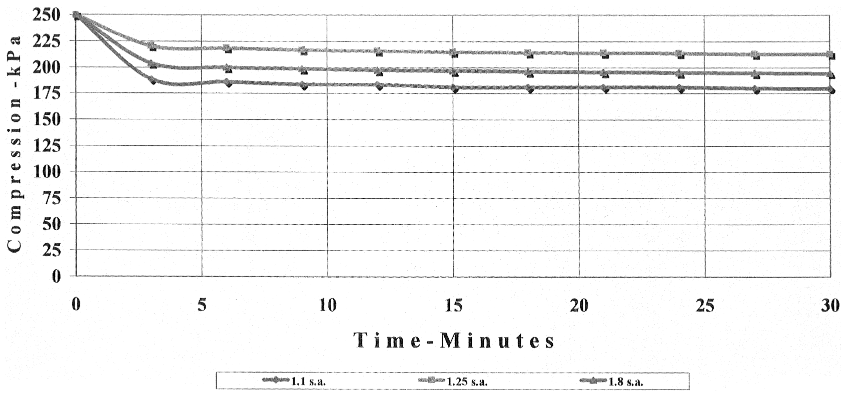

Fig. 6. Dry compression at 250 kPa.

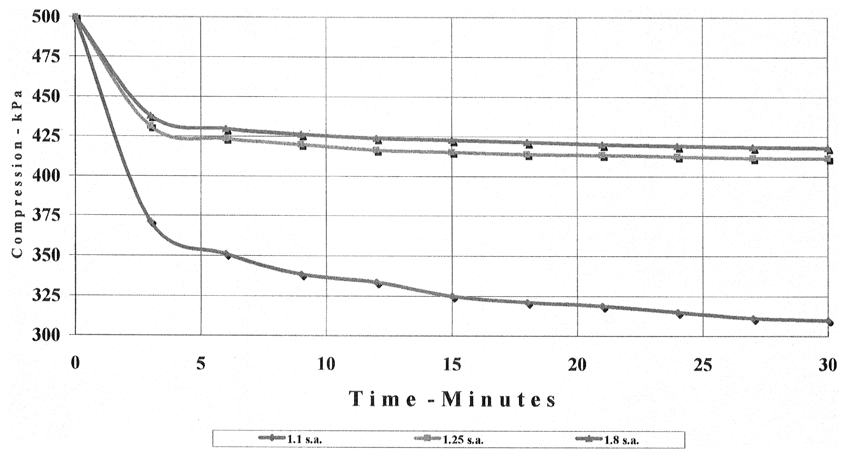

Fig. 7. Dry compression at 500 kPa.

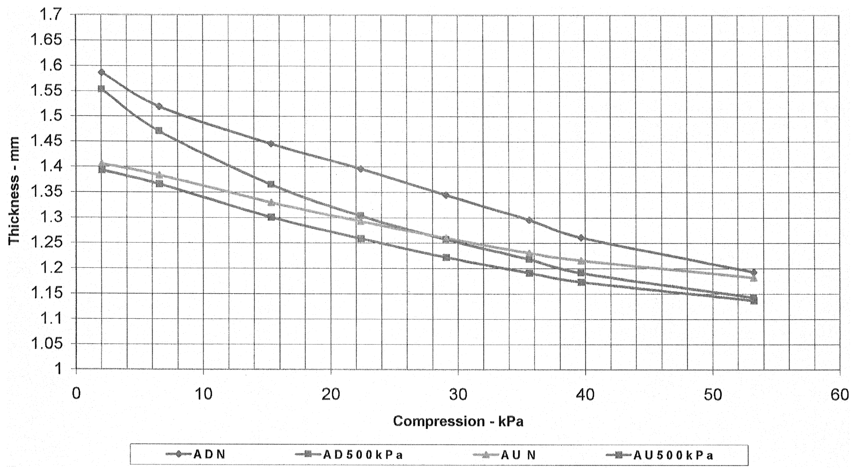

Fig. 8. Dry and wet BCI compression.

3.1.5. Compression behaviour

3.1.5.1. General. All samples showed the biggest drop in compression after the first 3 to 4 min of the test, after which point a gradual reduction or constant state is reached. This effect is discussed further under Section 3.2, Instrumentation, as the drop is observed with and without separator being present.

3.1.6. Compression—typical Trends—Hovosorb® separators

The 1.1 m^2/g surface area media at 100 and 250 kPa maintain a healthy level of compression, being comparable to the 1.25 m^2/g and 1.8 m^2/g samples. At 500 kPa, the ability of the 1.1 m^2/g media to maintain compression reduces well below its counterparts (Figs. 5–7).

The 1.25 m^2/g media performs better than the 1.8 m^2/g sheet under 100 and 250 kPa. At 500 kPa, the 1.8 m^2/g is better by a small margin. This result is a bit misleading, if taken out of context, as the 1.8 m^2/g sample was compressed at the faster rate of 10 mm/min for the 100 and 250 kPa tests, which showed a detrimental effect with tensile strength and elongations. However, even taking this into consideration, the 1.8 m^2/g sample would be hard-pushed to better the 1.25 m^2/g sample at the 100 and 250 kPa loading.

The 1.1 m^2/g media had a larger variability when compared with the 1.25 m^2/g media across the grammage range. This suggests that the extra surface area gives a benefit to the way the separator adsorbs and maintains the compressive forces applied.

The higher level of fine fibre in the 1.8 m^2/g sample does improve the compression resistance at 500 kPa, but not by a significant amount. Maybe, we do not need such a high surface area as 1.8 m^2/g. Somewhere between 1.25 m^2/g and 1.8 m^2/g would be the optimum.

There does not appear to be grammage dependence alone, on the ability to maintain the compressive force.

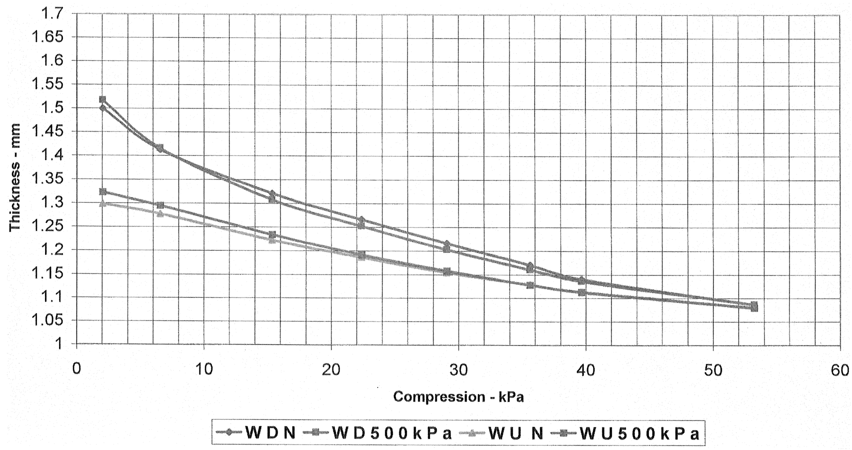

Fig. 9. Dry and wet BCI compression.

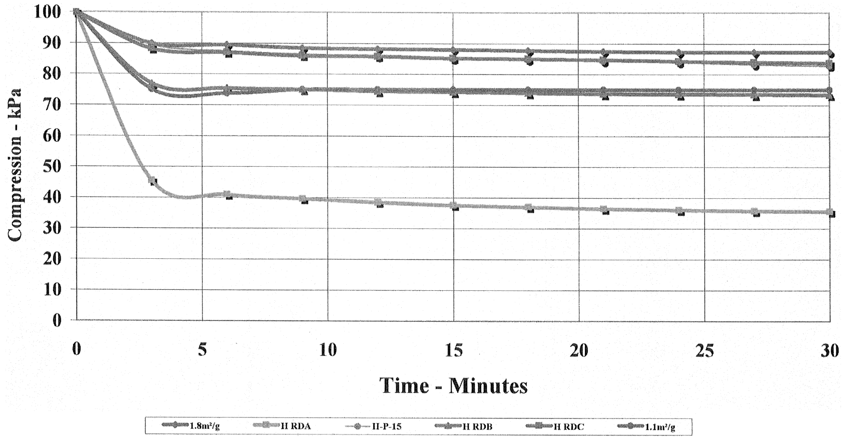

Fig. 10. Dry compression at 100 kPa.

The apparent density, grammage divided by the thickness, does, however, have an important effect. In simplistic terms, it indicates the amount of slack available within the separator to take up the compressive force. Having a fixed fibre blend rather than a variable fibre blend can also lead to a more consistent compression characteristic.

3.1.7. Additional compressive tests

The recovery after compression was calculated (2 kPa/500 kPa for 30 min/2 kPa).

The 1.1 m^2/g and 1.25 m^2/g RBSM separators recovered some 92% of their original thickness. The 1.8 m^2/g sample returned 96%. Considering the 500 kPa loading, the Standard Hovosorb® RBSM separators recover in a similar manner to that commonly associated with a 2-, 50-, 2-kPa test.

Standard dry and wet compression recovery curves [73] over the range of 2 to 53 kPa were generated for the 1.8 m^2/g sample (Figs. 8 and 9). Two samples were measured: a virgin sample—uncompressed, and a sample compressed to 500 kPa for 30 min.

The curves for the compressed and uncompressed samples are virtually carbon copies again, demonstrating the resilience of the standard RBSM.

3.1.8. Compression—typical trends—Modified Hovosorb® separators

The H RDA was significantly worse at 100 and 250 kPa than a standard RBSM separator but comparable at 500 kPa (Figs. 10–12).

The H RDB was comparable with the standard 1.1 m^2/g RBSM materials at 100 kPa and the 1.8 m^2/g RBSM material at 250 kPa. At 500 kPa, it was significantly better than all standard RBSM materials.

The H RDC maintained the highest level of compression at 100 and 250 kPa, being comparable with the best RBSM materials. At 500 kPa, its performance dropped that of below the 1.25 m^2/g and that of 1.8 m^2/g.

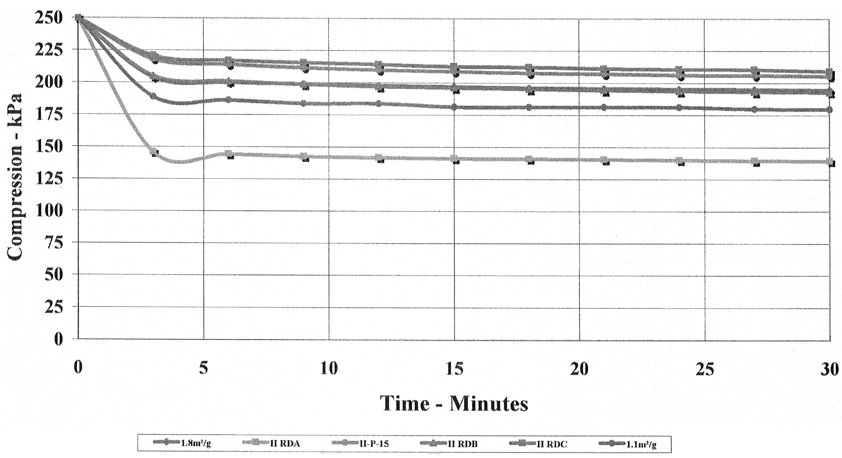

Fig. 11. Dry compression at 250 kPa.

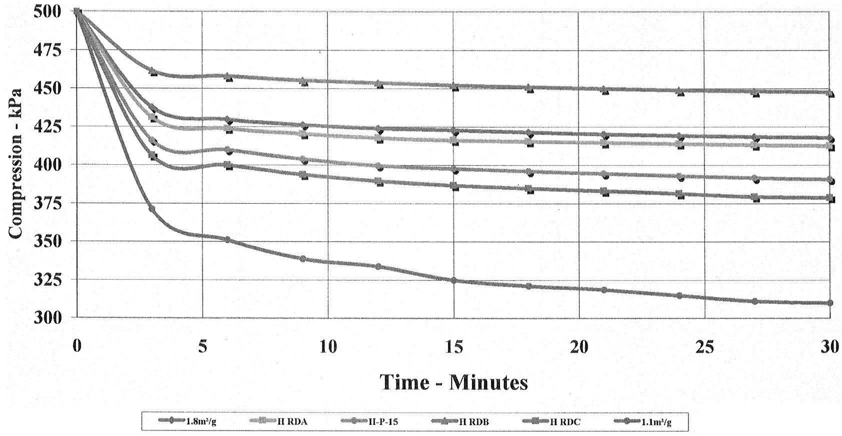

Fig. 12. Dry compression at 500 kPa.

The Hovosorb®-II-P-15 has similar good compression characteristics as the modified H RDC separator at 100 and 250 kPa. At 500 kPa, it held up slightly better than the H RDC.

3.1.9. Additional compressive tests

The recovery after compression was calculated (2 kPa/500 kPa for 30 min/2 kPa) for the Modified Hovosorb® RBSM materials. The modified separators returned between 94% and 91%. Again, a more than acceptable result considering the 500 kPa loading.

3.1.10. SEM

The SEM pictures showed little or no evidence of damage to the fibres for the 1.1 m^2/g, 1.25 m^2/g and H RDC. The 1.8 m^2/g, however, shows some breakage of the fibres. H RDA, H RDB and Hovosorb® II-P-15 have yet to be tested (Figs. 13 and 14).

Using the SEM to find breakage in the fibre is like looking for a needle in a haystack. Some 106 SEM pictures were taken at 250, 500 and 2000 magnification. Out of these, only five showed evidence of broken fibre. This equates to 4.7%. The breaks occurred: two with no loading, two 100-kPa loading and one with 500-kPa loading.

Additional tests on samples mounted on a sample holder, in the uncompressed state, then compressed and reviewed, showed that fibres are being reoriented within the matrix rather than breaking. This is certainly the trend shown by the images taken to date.

3.2. Instrumentation

The compression fixture was loaded into the Instron with the spacer plates and no separator. The 100, 250 and 500 kPa loading were maintained for a 30-min period and the observed change in force recorded to give a background reading for the instrumentation.

Independent of the force applied or speed used for the compression over the 30-min test period, the Instron, without the separators loaded into the test fixture (but compressed to the required force), dropped on average

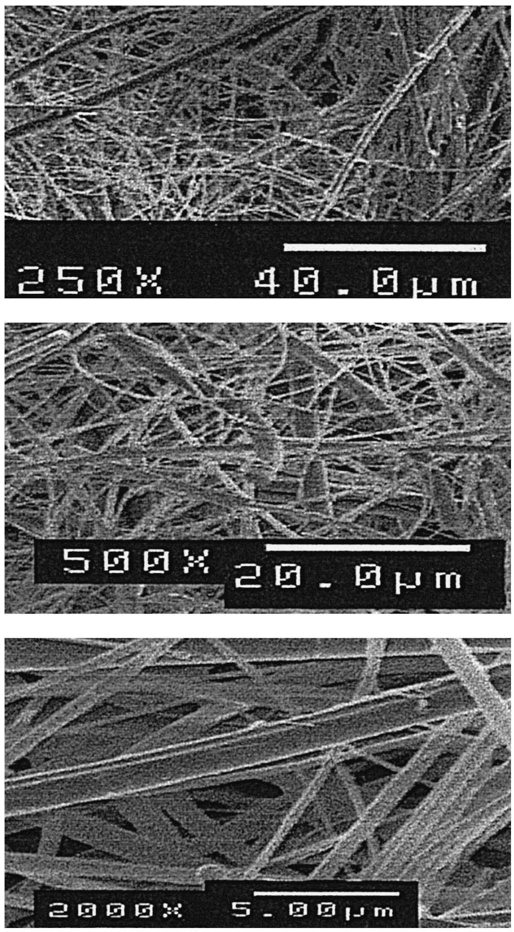

Fig. 13. Scanning electron microscope at 250×, 500×, and 2000× magnification.

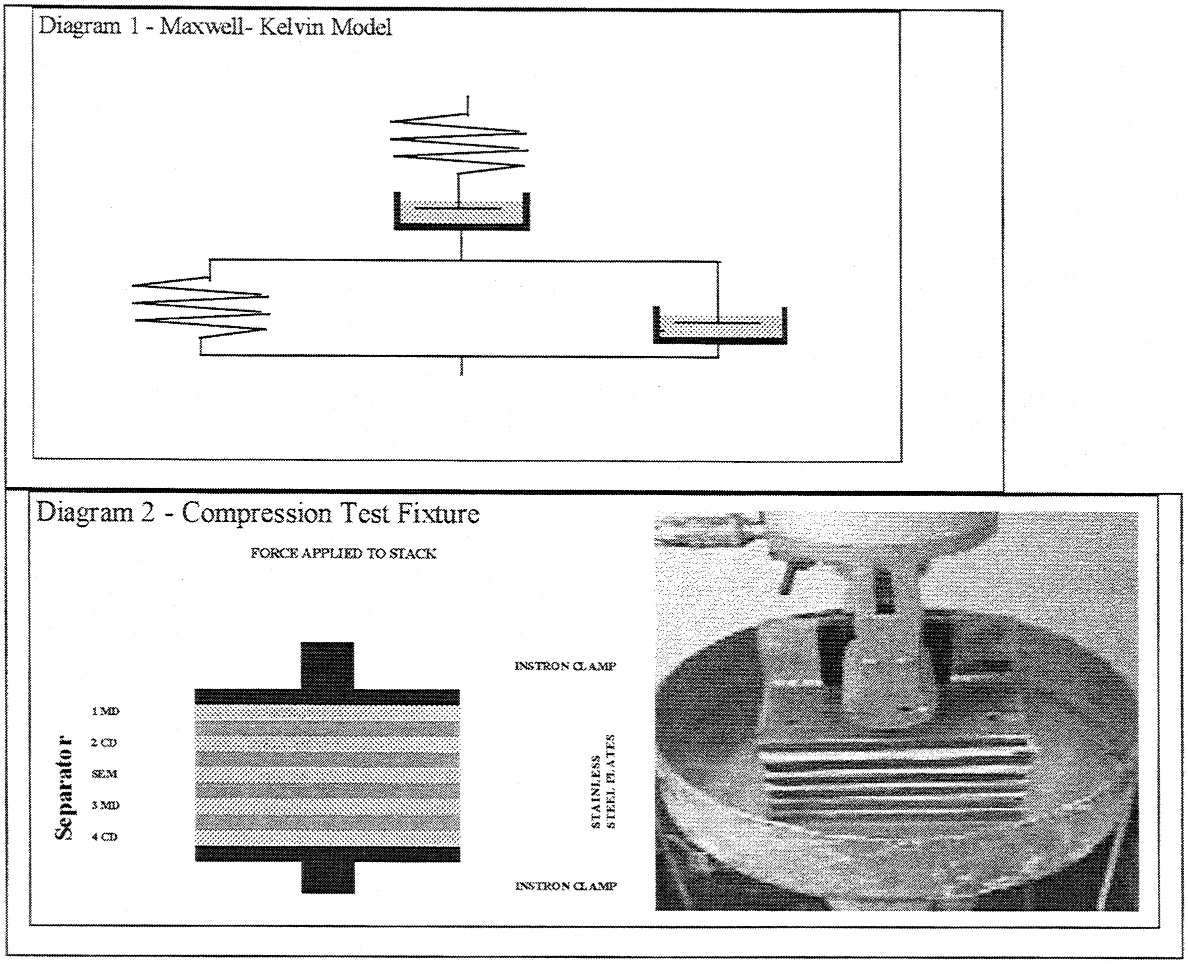

Fig. 14.

9.5%. In the first 3 min, the average drop was 6.5%, followed by a slight drop/plateau. This same trend was observed with the separator compression results.

This drop is believed to be damping within the electronics, electronic drift or some play in the test assembly. The drop was consistent on repetition.

Table 2
Drop in force

Reading	Separator	Average drop in force at 100 kPa		Average drop in force at 250 kPa		Average drop in force at 500 kPa	
		3 min (%)	30 min (%)	3 min (%)	30 min (%)	3 min (%)	30 min (%)
Original	1.1 m^2/g	31	36	17	20	26	38
Adjusted	1.1 m^2/g	25	27	10	11	19	28
Original	1.25 m^2/g	16	20	11	15	14	18
Adjusted	1.25 m^2/g	10	17	5	6	7	8
Original	1.8 m^2/g	30	36	18	22	13	16
Adjusted	1.8 m^2/g	24	26	12	13	6	7
Original	H RDA	55	64	42	44	13	17
Adjusted	H RDA	48	55	34	35	7	7
Original	H RDB	23	26	12	16	7	10
Adjusted	H RDB	16	17	5	6	2	1
Original	H RDC	12	16	12	16	19	24
Adjusted	H RDC	5	7	5	6	12	14
Original	II-P-15	10	17	13	18	17	22
Adjusted	II-P-15	4	8	6	8	10	12

Removing this background reading reduces the observed change in compressive force. There is still a drop inherent in the standard and modified RBSM separator, but significantly reduced. Table 2 shows the difference observed.

The previously reported HV study [72] will now be revisited to determine if the observed drop over the period of several days was mainly due to the instrumentation or separator.

4. Conclusion

To reduce and, ultimately, to overcome the problem of PCL2, higher levels of compression than those currently used will be required to keep the active material constrained.

The ability of RBSM separators to maintain compression resilience at higher applied forces has been answered by the findings within this report.

From the physical test results, it is clear that the Standard Hovosorb® RBSM separators, irrespective of surface area, are capable of handling compression forces up to 500 kPa.

The reduction in tensile strength and increase in elongation suggest that the matrix of the separator is changing as the force increases. The SEM study supports the concept of fibre displacement rather than fibre breakage with fibres moving in and out of the focal plain, rotating, spreading out and even grouping together.

Compression recoveries over 92% are observed for all Standard Hovosorb® RBSM separators (2 kPa/500 kPa for 30 min/2 kPa).

A snap shot dry/wet compression conducted on the 1.8 m^2/g separator shows that an uncompressed and a 500 kPa compressed separator show similar compressive behaviours.

From the physical test results, it is clear that the Modified Hovosorb® RBSM separators can enhance the basic character of a standard RBSM separator and improve its ability to handling compressive forces up to 500 kPa.

The best modified separators enhance the tensile strength of the standard RBSM, the II-P-15 maintains tensile strength across the range of applied forces, whilst the H RDC increases tensile strength across the range.

Compression recoveries of over 91% are observed for the Modified Hovosorb® RBSM separators (2 kPa/500 kPa for 30 min/2 kPa).

There is still life in the standard RBSM separator and benefits that can be added with the right modifier to enhance the properties further. Maintenance of compressive forces up to 500 kPa is well within the scope of current Hovosorb RBSM separator range.

It can be argued that the separator is not the weak link in the battery. The current limits are the battery design and methods of assembly.

Current thinking needs to take a step change, moving away from the skimpy box design and plates compressed in the region of 50 kPa, in the dry state, to more substantial cases and higher compression levels of 100 kPa and above. Methods of assembling with these forces will be required along with a closer understanding of what does and does not affect a separator during the assembly stage. Speed of compression at higher levels of compressive force is one area that can make or break a separator, for instance.

Acknowledgements

George Zguris—HV (WG) USA; Steve Downes—HV (WI) technician; Jeffrey Augostine—Analytical Answers—SEM driver; Lee Davis—HV (WI) workshop.

References

[1] U. Hullmeine, A. Winsel, E. Voss, J. Power Sources 25 (1989) 27.
[2] W. Borger, U. Hullmeine, H. Laig-Horstebrock, E. Meissner, in: T. Kelly, B.W. Baxter (Eds.), Power Sources, Proc. 16th Int. Power Source Symp., Vol. 12, 1988, pp. 131–145.
[3] E. Meissner, E. Voss, J. Power Sources 33 (1991) 231.
[4] E. Meissner, H. Rabenstein, J. Power Sources 40 (9) (1992) 157.
[5] E. Meissner, J. Power Sources 46 (1993) 231.
[6] C.P. Wales, A.C. Simon, J. Electrochem. Soc. 128 (1981) 2512.
[7] K. Harris, R.J. Hill, D.A.J. Rand, J. Power Sources 8 (1982) 175.
[8] J. Lee, J.F. Miller, C.C. Christianson, J. Power Sources 24 (1988) 215.
[9] K.R. Bullock, G.M. Trischan, R.G. Burrow, J. Electrochem. Soc. 130 (1983) 1283.
[10] K. Takahashi, N. Hoshihara, H. Yasuda, T. Ishii, H. Jimbo, J. Power Sources 30 (1990) 23.
[11] R.F. Nelson, D.M. Wisdom, J. Power Sources 33 (1991) 165.
[12] R. Peat, P.T. Moseley, L.T. Lam, D.A.J. Rand, J. Power Sources 38 (1992) 373.
[13] A.F. Hollenkamp, K.K. Constanti, A.M. Huey, M.J. Koop, L. Apateanu, J. Power Sources 40 (1992) 125.
[14] M.K. Dimitrov, D. Pavlov, J. Power Sources 46 (1993) 203.
[15] D. Pavlov, J. Power Sources 48 (1994) 179.
[16] R. Wagner, J. Power Sources 53 (1995) 153.
[17] P. Simon, N. Bui, N. Pebere, F. Dabosi, J. Power Sources 53 (1995) 63.
[18] P. Simon, N. Bui, N. Pebere, F. Dabosi, L. Albert, J. Power Sources 55 (1995) 63.
[19] S. Brinic, M. Metikos-Hukovic, R. Babic, J. Power Sources 55 (1995) 19.
[20] S. Tudor, A. Weisstuch, S.H. Davang, Electrochem. Technol. 5 (1967) 21.
[21] A. Winsel, E. Voss, U. Hullmeine, J. Power Sources 30 (1990) 209.
[22] A. Winsel, E. Voss, U. Hullmeine, DECHEMA Monogr. 121 (1990) 209.
[23] J. Burbank, J. Electrochem. Soc. 111 (1964) 1112.
[24] B.K. Mahato, J. Electrochem. Soc. 126 (1979) 365.
[25] J. Bohmann, U. Hullmeine, E. Voss, A. Winsel, ILZRO Project LE-277, Active material structure related to cycle life and capacity, Final Rep., Varta R&D, Dec. 1982.
[26] D. Pavlov, B. Monahov, G. Sundholm, T. Laitinen, J. Electroanal. Chem. 305 (1991) 57.
[27] E.M.L. Valeriote, A. Heim, M.S. Ho, J. Power Sources 33 (1991) 187.

[28] M. Calabek, P. Baca, V. Smarda, K. Micka, ALABC project AMC-003A, Final Rep., Brno Univ./J. Heyrovsky Inst., Aug. 1995.
[29] E. Meissner, J. Schulz, F.J. Glasner, D. Pavlov, G. Papazov, M. Bojinov, B. Monahov, T. Rogachev, St. Ruevski, ALABC project AMC-004, Final Rep., Varta R&D/CLEPS, Feb. 1995.
[30] D. Pavlov, G. Papazov, M. Bojinov, B. Monahov, T. Rogachev, St. Ruevski, ALABC project AMC-004A, CLEPS.
[31] T.G. Chang, J. Electrochem. Soc. 131 (1984) 1755.
[32] A.F. Hollenkamp, M.J. Koop, A.M. Huey, K.K. Constanti, J.A. Hamilton, L. Apateanu, L.H. Vu, CSIRO, ILZRO Project LE-371 Progress Rep. 4, 1992.
[33] A.F. Hollenkamp, M.J. Koop, K.K. Constanti, L. Apateanu, M. Calabek, K. Micka, J. Power Sources 48 (1994) 195.
[34] U. Hullmeine, E. Voss, A. Winsel, J. Power Sources 30 (1990) 99.
[35] E. Voss, A. Winsel, Yuasa-Jiho 68 (1990) 4.
[36] E. Voss, U. Hullmeine, A. Winsel, J. Power Sources 30 (1990) 33.
[37] E. Bashtavelova, A. Winsel, J. Power Sources 46 (1993) 219.
[38] E. Bashtavelova, A. Winsel, J. Power Sources 53 (1995) 175.
[39] F.J. Glasner, H. Kraft, E. Meissner, D. Metzeltin, J. Schulz, J. Vollbert, BRITE-EURAM project BE-7297, The development of improved lead-acid batteries for electric vehicle service which are maintenance-free and fully recyclable, task 4, First Annual Rep., Jan. 1995, and Second Annual Rep., Jan. 1996.
[40] V.E. Ruckborn, B. Witler, A. Winsel, DECHEMA Monogr. 102 (1986) 513.
[41] A. Winsel, E. Bashtavelova, J. Power Sources 46 (1993) 211.
[42] H. Hopfinger, A. Winsel, J. Power Sources 55 (1995) 143.
[43] T.G. Chang, in: K.R. Bullock, D. Pavlov (Eds.), Proc. Symp. Adv. Lead-Acid Batteries, Vol. 84-14, The Electrochemical Society, Pennington, NJ, USA, p. 86.
[44] L. Jumau, rev. d'Electricite, L'Eclairage E. R. J. Hill XVI (36) (1898) 413, lectrique.
[45] A.A. Cahen, L.H. Donaldson, The Electrician XLI (1898) 674.
[46] R.J. Hill, J. Power Sources 25 (1989) 313, and references therein.
[47] D. Pavlov, I. Balkanov, J. Electrochem. Soc. 139 (1992) 1830.
[48] D. Pavlov, J. Electrochem. Soc. 139 (1992) 3075.
[49] D. Pavlov, J. Power Sources 40 (1992) 169.
[50] D. Pavlov, J. Power Sources 46 (1993) 171.
[51] B. Monahov, D. Pavlov, J. Appl. Electrochem. 23 (1993) 1244.
[52] D. Pavlov, J. Power Sources 53 (1995) 9, and references therein.
[53] K. Takahashi, M. Tsubota, K. Yonezu, K. Ando, J. Electrochem. Soc. 130 (1983) 2144.
[54] J. Alzieu, J. Robert, J. Power Sources 13 (1984) 93.
[55] J. Alzieu, N. Koechlin, J. Robert, J. Power Sources 134 (1987) 1881.
[56] P. Ruetschi, J. Electrochem. Soc. 139 (1992) 1347.
[57] Y. Okada, K. Takahashi, M. Tsubota, GS 52 (1993) 13, EVS11.
[58] K.K. Constanti, A.F. Hollenkamp, M.J. Koop, K. McGregor, CSIRO, ALABC project AMC-003, Final Rep., May 1995.
[59] K.K. Constanti, A.F. Hollenkamp, M.J. Koop, K. McGregor, J. Power Sources 55 (1995) 269.
[60] A.F. Hollenkamp, J. Power Sources 36 (1991) 567.
[61] A.F. Hollenkamp, J. Power Sources 67 (1997) 27.
[62] R.F. Nelson, D.A.J. Rands (Eds.), Proc. 1st Meet, The ALABC PCL Study Group, ILZRO, 23rd Sept. 1993.
[63] R.F. Nelson, D.A.J. Rands (Eds.), Proc. 2nd Meet, The ALABC PCL Study Group, ILZRO, 19th Sept. 1994.
[64] A.F. Hollenkamp, J. Power Sources 59 (1996) 87.
[65] K. Takahashi, M. Tsubota, K. Yoneza, K. Ando, J. Electrochem. Soc. 130 (1983) 2144.
[66] J. Landfors, J. Power Sources 52 (1994) 99.
[67] S. Atlung, B. Zachau-Christiansan, J. Power Sources 30 (1990) 131.
[68] J. Alzieu, B. Geoffrion, N. Lexaude, J. Robert, Proc. EVS5, 2nd Oct. 1978.
[69] D. Pavlov, J. Power Sources 33 (1991) 221.
[70] E. Meissner, J. Power Sources 67 (1997) 135.
[71] V. John, Intro. Eng. Mater., 3rd edn., Chap. 9, Macmillan, London, ISBN 0333568273.
[72] G. Zguris, J. Power Sources 67 (1997) 307.
[73] BCI compression test, II34-1.
[74] JIS thickness test, JIS C2202, 1971.